Frequency-Domain Ultrasound Waveform Tomography Breast Attenuation Imaging

Gursharan Yash Singh Sandhu[a,b], Cuiping Li[a,b], Olivier Roy[a,b], Erik West[a], Katelyn Montgomery[a], Neb Duric[a,b];

[a]Delphinus Medical Technologies, USA;

[b]Karmanos Cancer Institute, USA

ABSTRACT

Ultrasound waveform tomography techniques have shown promising results for the visualization and characterization of breast disease. By using frequency-domain waveform tomography techniques and a gradient descent algorithm, we have previously reconstructed the sound speed distributions of breasts of varying densities with different types of breast disease including benign and malignant lesions. By allowing the sound speed to have an imaginary component, we can model the intrinsic attenuation of a medium. We can similarly recover the imaginary component of the velocity and thus the attenuation. In this paper, we will briefly review ultrasound waveform tomography techniques, discuss attenuation and its relations to the imaginary component of the sound speed, and provide both numerical and *in vivo* examples of waveform tomography attenuation reconstructions.

Preferred Presentation Type: Oral presentation

Keywords: attenuation, breast cancer, clinical breast imaging, quantitative imaging, waveform tomography

1. DESCRIPTION OF PURPOSE

Ultrasound techniques have been successful in detecting and classifying breast disease.[1] By incorporating the principles of tomography with a ring array ultrasound transducer array, ultrasound tomography has led to new developments in breast imaging.[2,3] The technique is capable of producing typical B-mode reflection images in addition to quantifying the sound speed and attenuation properties of a breast by using ray based techniques.[4,5] In contrast to ray techniques, frequency-domain waveform tomography techniques more accurately model the physics of wave propagation. This has allowed gradient descent inversion algorithms to reconstruct more accurate sound speed distributions of the insonified medium by iteratively minimizing a cost function defined as the difference between real and synthetically generated acoustic pressure fields.[6–10] By allowing the sound speed to have an imaginary part, one is able to model the intrinsic attenuation of a medium.[11] Since the attenuation, in addition to sound speed, can characterize different types of lesions,[12] it is hoped that frequency-domain ultrasound waveform tomography attenuation imaging can aid in the classification of breast disease in a clinical setting.

2. METHOD

We solve the Helmholtz equation for complex sound speed by using finite difference methods to model the Helmholtz operator, and we use gradient descent methods to update a complex valued sound speed by minimizing the difference between forward modeled and inverse modeled acoustic pressure data. Further details about the data acquisition and reconstruction process can be found in our previous publications.[8–10]

In the typical diagnostic range of 0.5 - 10 MHz, the acoustic attenuation of ultrasound waves in soft tissue is approximately linearly dependent on the frequency.[12,13] We also assume there is no dispersion of the acoustic phase velocity. Therefore, if we divide by the frequency and distance, we can obtain an attenuation coefficient α of ultrasound attenuation in units of dB/(mm·MHz). This type of unit is the most quoted unit in discussion regarding to ultrasound attenuation. In order to tie this with concept of imaginary sound speed, we will discuss

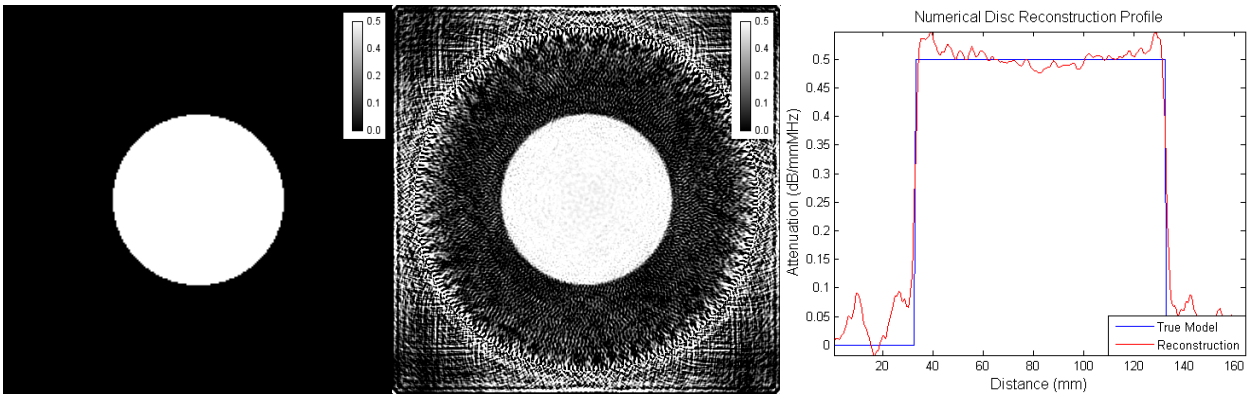

(a) (b) (c)

Figure 1: Numerical simulation of 0.5 dB/(mm·MHz) 50 mm attenuation disc. Sound speed constant at 1500 m/s. Overlay bar in units of dB/(mm·MHz) included. (a) True model; (b) Reconstructed α; (c) Plot profile.

the quality factor Q. A detailed discussion is available in Aki and Richards.[11] The quality factor Q is defined in terms of the energy loss ΔE in a cycle of a plane wave oscillating at frequency ω

$$\frac{1}{Q} = -\frac{\Delta E}{2\pi E}\,.$$

Thus, the amplitude $A(x)$ at a position x of a plane wave with initial amplitude A_0 oscillating at a frequency ω in a medium with complex velocity $c = c_R + c_I$ and quality factor Q is given by

$$A(x) = A_0 \exp\left[\frac{-\omega x}{2c_R Q}\right], \qquad c_I = \frac{c_R}{2Q}\,.$$

where c_R is the phase velocity and c_I is proportional to attenuation. The attenuation coefficient α is then

$$\alpha = \frac{20}{\ln 10}\frac{2\pi c_I}{c_R^2}\,.$$

Thus, by inverting acoustic data and reconstructing the parameter c_I we can obtain attenuation in units of dB/(mm·MHz). We will do this process using numerical simulations and show how close our reconstruction is to the true model by using line profiles. We will also show a preliminary *in vivo* attenuation image.

3. RESULTS

In Figure 1, we see the numerical simulation reconstruction of a 50 mm disc with $\alpha = 0.5$ dB/(mm·MHz). The sound speed was held constant at 1500 m/s. The reconstruction used frequencies between 200 and 710 kHz with a frequency interval of 30 kHz. We see that the algorithm did an excellent job of recovering the attenuation coefficient α. However, the ripples in the plot profile shows the recovery of the attenuation parameter is not as well conditioned as the recovery of sound speed.[8] We suspect that instability at low frequencies may be the cause. A Gaussian blur with a standard deviation of 0.5 was applied to the line profile to suppress rippiling.

In Figure 2, we see the numerical simulation reconstruction of a breast phantom. It is comprised of a skin layer, subcutaneous fat layer, soft tissue layer, and embedded high attenuation and low attenuation lesions. The attenuation of these structures are 0.25, 0.05, 0.15, 0.50, and 0.05 dB/(mm·MHz), respectively. The size, shape, and attenuation values are set to simulate a real breast. The sound speed was held constant at 1500 m/s. The reconstruction used frequencies between 500 and 1010 kHz with a frequency interval of 30 kHz. The attenuation reconstruction of the numerical breast phantom is not as close to the true model when compared to the disc phantom. However, it is significantly more complicated with varying contrast between different lesions and tissues. It can be seen that the skin layer is well resolved and that high resolution features, such as the

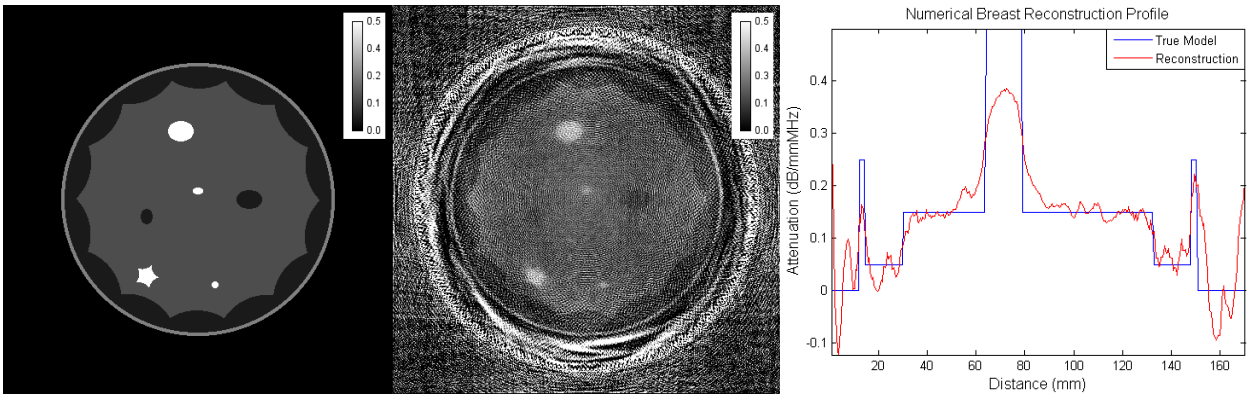

(a) (b) (c)

Figure 2: Numerical simulation of breast. Sound speed constant at 1500 m/s. Overlay bar in units of dB/(mm·MHz) included. (a) True model; (b) Reconstructed α; (c) Plot profile.

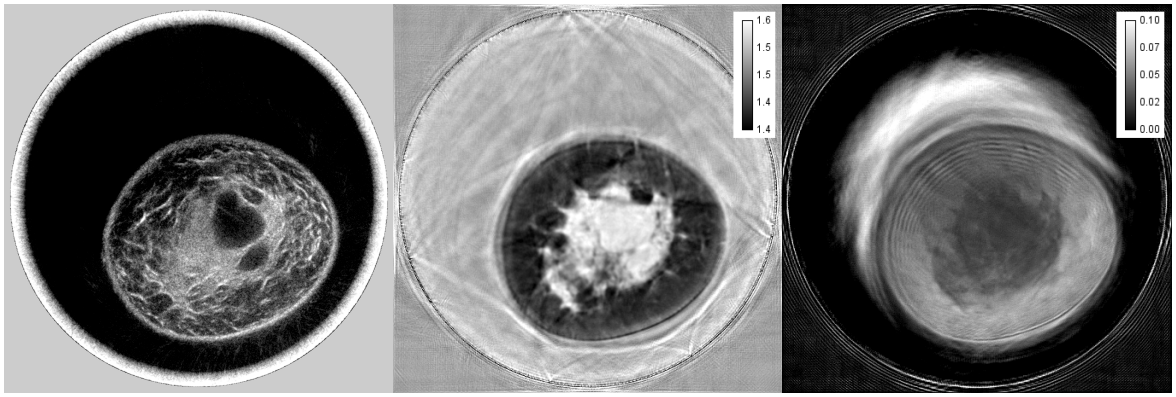

(a) (b) (c)

Figure 3: *In vivo* breast reconstruction. Overlay bar in units of mm/μs included. (a) B-Mode reconstruction. (a) Real sound speed reconstruction; (b) Imaginary sound speed reconstruction.

cascading of the glandular tissue into the subcutaneous fat layer, the small high attenuation lesions, and the star shape of the high attenuation lesion, are well resolved. A difficult task for the attenuation reconstruction is resolving low attenuation contrast. In Figure 2c, we see a horizontal line profile across the high attenuation lesion at 12 o'clock. It is seen that the algorithm has matched the attenuation of the various lesions types to some degree of accuracy, but like the attenuation disc, there is rippiling in the line profile. Thus, we conclude that it will be necessary to incorporate some type of regularization or filtering of the gradient map to improve the image. Additionally, we need to reconstruct an optimal set of frequencies to more accurately match the true model. A Gaussian blur with a standard deviation of 0.5 was applied to the line profile to suppress rippiling.

In Figure 3, we see *in vivo* reconstruction of a breast with a cyst. The sound speed reconstruction used frequencies between 500 and 1010 kHz with a frequency interval of 30 kHz, while the attenuation reconstruction only used one frequency at 1010 kHz. The sound speed model was determined first using amplitude normalized data. The attenuation image was then reconstructed using data normalized with respect to its magnitude in water. Note that we show the imaginary part of sound speed c_I so that it is clear that the structures being imaged are not simply carried over by the sound speed reconstruction. A B-mode reflection and sound speed image are included in Figure 3 to highlight the cyst location. From viewing the *in vivo* result, it is encouraging that we can recover, for example, the outer contours of the breast and the differentiation of tissues in the interior of the breast. However, it is problematic that innermost part of the breast is not higher attenuating then the outer fatty portion as would be expected. In addition, there is no dark spot of low attenuation as would be expected for the cyst location. There is also a high attenuation artifact outside the breast in the water.

4. NEW OR BREAKTHROUGH WORK TO BE PRESENTED

We present waveform tomography attenuation images using numerical simulations and the inversion of *in vivo* data. This work is important because the transmission properties of tissues can help in the classification and diagnosis of breast disease. It is also important because waveform tomography sound speed imaging has shown to improve the assessment of breast sound speed over ray methods. We have shown simulation results and preliminary *in vivo* results which uses a simple water normalization procedure. By incorporating additional appropriate preprocessing of the data, we hope to significantly improve the clinical diagnostic value of waveform tomography attenuation images.

5. CONCLUSIONS

Our simulation results show that our waveform tomography algorithm is capable of recovering the attenuation properties of tissues. Our preliminary *in vivo* results with a simple water magnitude normalization shows that the algorithm is capable of recovering the outer contours of the breast as well as detailed morphological information in the interior of the breast. However, we question the validity of recovered attenuation values as they do not obey what we would expect from our experience and published research. We emphasize these results are preliminary, and that we expect major improvements as we improve the preprocessing of the data and implement changes to the algorithm. This work has not been published elsewhere.

REFERENCES

[1] Stavros, A. T., Thickman, D., Rapp, C. L., Dennis, M. A., Parker, S. H., and Sisney, G. A., "Solid breast nodules: use of sonography to distinguish between benign and malignant lesions.," *Radiology* **196**(1), 123–134 (1995).

[2] Duric, N., Littrup, P., Poulo, L., Babkin, A., Pevzner, R., Holsapple, E., Rama, O., and Glide, C., "Detection of breast cancer with ultrasound tomography: First results with the computed ultrasound risk evaluation (CURE) prototype," *Medical physics* **34**(2), 773–785 (2007).

[3] Duric, N., Littrup, P., Schmidt, S., Li, C., Roy, O., Bey-Knight, L., Janer, R., Kunz, D., Chen, X., Goll, J., et al., "Breast imaging with the softvue imaging system: First results," in [*SPIE Medical Imaging*], 86750K–86750K, International Society for Optics and Photonics (2013).

[4] Li, C., Duric, N., and Huang, L., "Clinical breast imaging using sound-speed reconstructions of ultrasound tomography data," in [*Medical Imaging*], 692009–692009, International Society for Optics and Photonics (2008).

[5] Li, C., Duric, N., and Huang, L., "Comparison of ultrasound attenuation tomography methods for breast imaging," in [*Medical Imaging*], 692015–692015, International Society for Optics and Photonics (2008).

[6] Pratt, R. G., "Seismic waveform inversion in the frequency domain, part 1: Theory and verification in a physical scale model," *Geophysics* **64**(3), 888–901 (1999).

[7] Pratt, R. G., Huang, L., Duric, N., and Littrup, P., "Sound-speed and attenuation imaging of breast tissue using waveform tomography of transmission ultrasound data," in [*Medical Imaging*], 65104S–65104S, International Society for Optics and Photonics (2007).

[8] Li, C., Sandhu, G. S., Roy, O., Duric, N., Allada, V., and Schmidt, S., "Toward a practical ultrasound waveform tomography algorithm for improving breast imaging," in [*SPIE Medical Imaging*], 90401P–90401P, International Society for Optics and Photonics (2014).

[9] Sandhu, G. Y., Li, C., Roy, O., Schmidt, S., and Duric, N., "High-resolution quantitative whole-breast ultrasound: in vivo application using frequency-domain waveform tomography," in [*SPIE Medical Imaging*], 94190D–94190D, International Society for Optics and Photonics (2015).

[10] Sandhu, G., Li, C., Roy, O., Schmidt, S., and Duric, N., "Frequency domain ultrasound waveform tomography: breast imaging using a ring transducer," *Physics in medicine and biology* **60**(14), 5381 (2015).

[11] Aki, K. and Richards, P. G., [*Quantitative seismology*], vol. 1 (2002).

[12] Duck, F. A., [*Physical properties of tissues: a comprehensive reference book*], Academic press (2013).

[13] Sushilov, N. V. and Cobbold, R. S., "Frequency–domain wave equation and its time–domain solutions in attenuating media," *The Journal of the Acoustical Society of America* **115**(4), 1431–1436 (2004).